Constraining the helium abundance with CMB data

Trotta, Roberto; Hansen, Steen H.

Constraining the helium abundance with CMB data

Roberto Trotta*
Département de Physique Théorique, Université de Genève, 24 quai Ernest Ansermet, CH-1211 Genève 4, Switzerland

Steen H. Hansen†
Physik Institut, Winterthurerstrasse 190, 8057 Zurich, Switzerland

(Received 10 July 2003; published 30 January 2004)

We consider for the first time the ability of present-day cosmic microwave background (CMB) anisotropies data to determine the primordial helium mass fraction Y_p. We find that CMB data alone give the confidence interval $0.160<Y_p<0.501$ (at 68% C.L.). We analyze the impact on the baryon abundance as measured by CMB and discuss the implications for big bang nucleosynthesis. We identify and discuss correlations between the helium mass fraction and both the redshift of reionization and the spectral index. We forecast the precision of future CMB observations, and find that Planck alone will measure Y_p with error bars of 5%. We point out that the uncertainty in the determination of the helium fraction will have to be taken into account in order to correctly estimate the baryon density from Planck-quality CMB data.

DOI: 10.1103/PhysRevD.69.023509 PACS number(s): 98.80.−k, 04.50.+h, 95.35.+d, 98.70.Vc

I. INTRODUCTION

Our understanding of the baryon abundance has increased dramatically over the past few years. This improvement comes from two independent paths: namely, big bang nucleosynthesis (BBN) and cosmic microwave background (CMB) radiation. Absorption features from high-redshift quasars allow us to measure precisely the deuterium abundance, D/H. Combined with BBN calculations, this provides a reliable estimate of the baryon to photon ratio, η. An independent determination of the baryon content of the Universe from CMB anisotropies comes from the increasingly precise measurements of the acoustic peaks, which bear a characteristic signature of the photon-baryon fluid oscillations. The agreement between these two completely different approaches is both remarkable and impressive (see details below). The time is therefore ripe to proceed and test the agreement between other light elements which are also probed both with BBN and CMB.

The helium abundance has been measured for many years from astrophysical systems. However, the error bars are seemingly dominated by systematic errors which are hard to assess. Fortunately, the dependence of the helium mass fraction on the CMB anisotropies provides an independent way to measure Y_p. The aim of this work is to present the first determination of the helium abundance from CMB alone, and to clarify the future potential of this method. The latest CMB data are precise enough to allow taking this further step, and in view of the emerging ''baryon tension'' between BBN predictions from observations of different light elements [1] possibly requires taking such a step. The advantage of using CMB anisotropies rather than the traditional astrophysical measurements, is that CMB provide a clear measurement of the primordial helium fraction before it could be changed by any astrophysical process. On the other hand the dependence of the CMB power spectrum on Y_p is rather mild, a fact which makes it presently safe to fix the value of the helium mass fraction with zero uncertainty for the purpose of CMB data analysis of other cosmological parameters.

The paper is organized as follows. In Sec. II we review the standard big bang nucleosynthesis scenario. Sec. III discusses the role of the helium mass fraction for cosmic microwave background anisotropies, the methods used and results. We discuss our forecast for future CMB observations in Sec. III D, and offer our conclusions in Sec. IV.

II. BIG BANG NUCLEOSYNTHESIS

A. The standard scenario

The standard model of big bang nucleosynthesis (SBBN) has only one free parameter, namely the baryon to photon ratio $\eta_{10}=n_b/n_\gamma 10^{10}$, which for long has been known to be in the range 1–10 [2]. Thus by observing just one primordial light element one can predict the abundances of all the other light elements.

The deuterium to hydrogen abundance, D/H, is observed by Ly-α features in several quasar absorption systems at high redshift, $\mathrm{D/H}=2.78^{+0.44}_{-0.38}\times 10^{-5}$ [3], which in SBBN translates into the baryon abundance, $\eta_{10}=5.9\pm 0.5$. Using SBBN one thus predicts the helium mass fraction to be in the range $0.2470<Y_p<0.2487$. The dispersion in various deuterium observations is, however, still rather large, ranging from $\mathrm{D/H}=1.65\pm 0.35\times 10^{-5}$ [4] to $\mathrm{D/H}=3.98^{+0.59}_{-0.67}\times 10^{-5}$ [3], which most probably indicates underestimated systematic errors.

The observed helium mass fraction comes from the study of extragalactic H II regions in blue compact galaxies. One careful study [5] gives the value $Y_P=0.244\pm 0.002$; however, also here there is a large scatter in the various observed values, ranging from $Y_p=0.230\pm 0.003$ [6] over $Y_p=0.2384\pm 0.0025$ [7] and $Y_p=0.2391\pm 0.0020$ [8] to $Y_p=0.2452\pm 0.0015$ [9]. Besides the large scatter there is also

*Electronic address: roberto.trotta@physics.unige.ch
†Electronic address: hansen@physik.unizh.ch

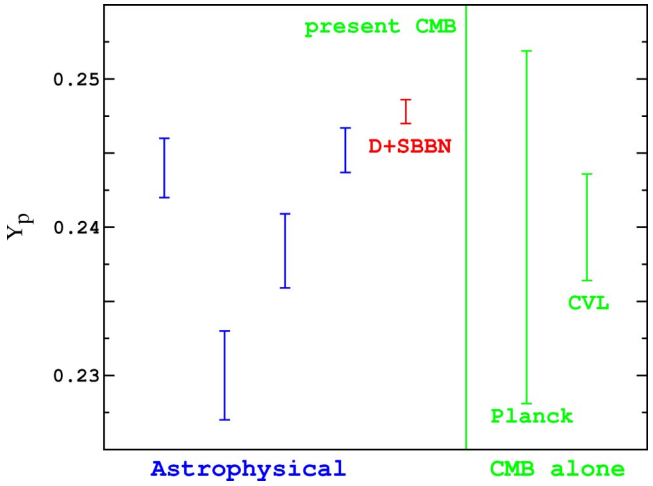

FIG. 1. On the left (blue) we plot a few current direct astrophysical measurements of the helium mass fraction Y_p with their $1-\sigma$ statistical errors, and the value inferred from deuterium measurements combined with SBBN (red) (see text for references). On the right (green), a direct comparison with CMB present-day accuracy (actual data, this work; the error bar extends in the range $0.16<Y_p<0.50$) and with its future potential (Fisher matrix forecast for Planck and a cosmic variance limited experiment).

the problem that the helium mass fraction predicted from observation of deuterium combined with SBBN, $0.2470<Y_p<0.2487$, is larger than (and seems almost in disagreement with) most of the observed helium abundances, which probably points towards underestimated systematic errors, rather than the need for new physics [1,10]. Figure 1 is a compilation of the above measurements, and offers a direct comparison with the current (large) errors from CMB observations (presented in Sec. III below) and with the potential of future CMB measurements (discussed in Sec. III D).

The observed abundance of primordial ^{7}Li using the Spite plateau is possibly spoiled by various systematic effects [11,12]. Therefore it is more appropriate to use the SBBN predictions together with observations to estimate the depletion factor $f_7=^7\mathrm{Li}_{\mathrm{obs}}/^7\mathrm{Li}_{\mathrm{prim}}$ instead of using $^7\mathrm{Li}_{\mathrm{obs}}$ to infer the value of η [14–17].

The numerical predictions of standard BBN (as well as various nonstandard scenarios) have reached a high level of accuracy [13,14,18–21], and the precision of these codes is well beyond the systematic errors discussed above.

B. The role of neutrinos

If the CMB-determined helium mass fraction turns out to be as high as suggested by SBBN calculations combined with the observed deuterium abundance (as discussed above), this could indicate a systematic error in the present direct astrophysical helium observations. Alternatively, if the CMB could independently determine the helium value with sufficient precision to confirm the present low helium value coming from direct observations, then this would be a smoking gun for new physics. In fact, one could easily imagine nonstandard BBN scenarios which would agree with present observations of η_{10}, while having a low helium mass fraction. All that is needed is additional nonequilibrium electron neutrinos produced at the time of neutrino decoupling which would alter the $n-p$ reaction. This could alter the resulting helium mass fraction while leaving the deuterium abundance unchanged. One such possibility would be a heavy sterile neutrino whose decay products include ν_e. A sterile neutrino with lifetime of 1–5 sec and with decay channel $\nu_s\rightarrow\nu_e+\phi$ with ϕ a light scalar (like a majoron), would leave the deuterium abundance roughly untouched, but can change the helium mass fraction between $\Delta Y_p=-0.025$ and $\Delta Y_p=0.015$ if the sterile neutrino mass is in the range 1–20 MeV [22]. A simpler model would be standard neutrino oscillation between a sterile neutrino and the electron neutrino. The lifetime is about 1 sec when the sterile state has mass about 10 MeV, and the decay channel is $\nu_s\rightarrow\nu_e+l+\bar{l}$ (with l any light lepton), and such masses and lifetimes are still unconstrained for large mixing angle [23] (related BBN issues are discussed in Refs. [24–27]). Such possibilities are hard to constrain without an independent measurement of the helium mass fraction.

Another much studied effect of neutrinos is the increased expansion rate of the universe if additional degrees of freedom are present (for BBN), and the degeneracy between the total density in matter and relativistic particles (for CMB). This issue has recently been studied in detail in Refs. [10,28] in view of the new WMAP results, and we need not discuss this further here. We thus fix $N_\nu=3.04$ [29]. Also an electron neutrino chemical potential could potentially alter the BBN predictions [30], however, with the observed neutrino oscillation parameters the different neutrino chemical potentials would equilibrate before the onset of BBN [31], hence virtually excluding this possibility (see however [32]).

III. COSMIC MICROWAVE BACKGROUND

A. Photon recombination and reionization

The recent WMAP data allow one to determine with very high precision the epoch of photon decoupling, z_{dec}, i.e., the epoch at which the ionized electron fraction, $x_e(z)=n_e/n_H$, has dropped from 1 to its residual value of order 10^{-4}. Here n_e denotes the number density of free electrons, while n_H is the total number density of H atoms (both ionized and recombined). After this moment, photons are no longer coupled to electrons (last scattering), and they free stream. The redshift of decoupling has been determined to be $z_{\mathrm{dec}}=1088^{+1}_{-2}$ [33], which corresponds to a temperature of about 0.25 eV. Helium recombines earlier than hydrogen, roughly in two steps: around redshift $z=6000$ He III recombines to He II, while He II to He I recombination begins around $z<2500$ and finishes just after the start of H recombination (see e.g. [34–37]).

Denoting by n_{He} and n_b the number densities per m^3 of He atoms and baryons, respectively, the helium mass fraction is defined as $Y_p=4n_{He}/n_b$. The baryon number density is related to the baryon energy density today, ω_b, by $n_b=11.3(1+z)^3\omega_b$ and we have $n_H=n_b(1-Y_p)$. Usually, the ionization history is described in terms of $x_e(z)=n_e/(n_b(1-Y_p))$. However, for the purpose of discussing the role of

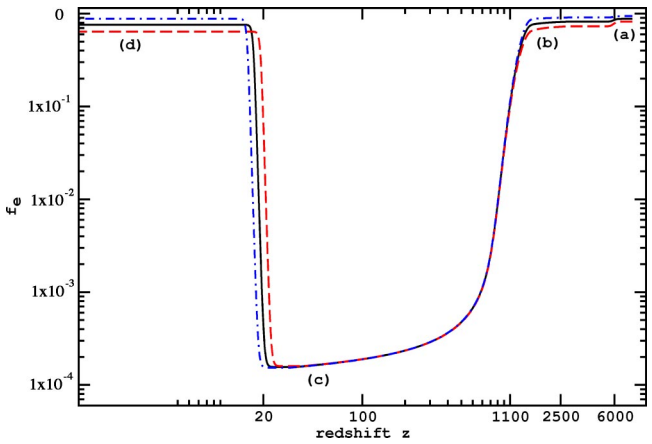

FIG. 2. Evolution of the number density of electrons normalized to the number density of baryons, $f_e = n_e/n_b$, as a function of redshift for different values of the helium fraction Y_p. The black-solid curve corresponds to the standard value $Y_p = 0.24$, and the red-dashed (blue-dot-dashed) curve to $Y_p = 0.36$ ($Y_p = 0.12$). The labels (a) to (d) indicate the four different phases discussed in the text.

Y_p, it is more convenient to consider the quantity $f_e(z) = n_e/n_b$ instead, the ratio of free electrons to the total number of baryons. For brevity, we will call f_e the free electron fraction. Once the baryon number density has been set by fixing ω_b, one can think of Y_p as an additional parameter which controls the number of free electrons available in the tight coupling regime. The CMB power spectrum depends on the full detailed evolution of the free electron fraction, but we can qualitatively describe the role of helium in four different phases of the ionization-recombination history (see Fig. 2).

(a) Before He III recombination all electrons are free, therefore $f_e(z > 6000) = 1 - Y_p/2$.

(b) He II progressively recombines and just before H recombination begins, f_e has dropped to the value $f_e(z \approx 1100) = 1 - Y_p$.

(c) After decoupling, a residual fraction of free electrons freezes out, giving $f_e(30 \lesssim z \lesssim 800) = f_e^{\rm res} \approx 2.7 \times 10^{-5} \sqrt{\omega_m}/\omega_b$.

(d) Reionization of all the H atoms gives $f_e(z \lesssim 20) = 1 - Y_p$.

During phase (a), the photon-baryons fluid is in the tight coupling regime. However the presence of ionized He increases diffusion damping, therefore having an impact on the damping scale in the acoustic peaks region. When the detailed energy levels structure of He II is taken into account [37], the transition to phase (b) is smoother than in the Saha equation approximation. Therefore the plateau with $f_e = 1 - Y_p$ is not visible in Fig. 2. Before H recombination, He atoms remain tightly coupled to H atoms through collisions, with the same dynamical behavior. In particular, it is the total ω_b which determines the amount of gravitational pressure on the photon-baryons fluid, and which sets the acoustic peak enhancement or suppression. Hence we do not expect the value of Y_p to have any influence on the boosting (suppression) of odd (even) peaks. The redshift of decoupling [transition between (b) and (c)] depends mildly on Y_p in a correlated way with ω_b, since the number density of free electrons in the tight coupling regime (just before H recombination) scales as $n_e = f_e n_b = n_b(1 - Y_p)$. Hence an increase in ω_b can be compensated by allowing for a larger helium fraction. An analytical estimate along the same lines as in e.g. [2] indicates that a 10% change in Y_p affects $z_{\rm dec}$ by roughly 0.1%, which corresponds to $\Delta z_{\rm dec} \approx 1$. This is of the same order as the current 1σ errors on $z_{\rm dec}$, obtained by fixing $Y_p = 0.24$.

After H recombination, the residual ionized electron fraction $f_e^{\rm res}$ does not depend on Y_p, but is inversely proportional to the total baryon density [phase (c)]. As the CMB photons propagate, they are occasionally rescattered by the residual free electrons. The corresponding optical depth, $\tau^{\rm res}$ is given by

$$\tau^{\rm res} = \int_{t_0}^{t_{\rm dec}} n_e^{\rm res} c \sigma_T dt \approx 1.86 \times 10^{-6} \int_0^{z_{\rm dec}} \frac{(1+z)^2}{((1+z)^3 + \Omega_\Lambda/\Omega_m)^{1/2}} dz. \quad (1)$$

Performing the integral we can safely neglect the contribution of the cosmological constant at small redshift, since $z_{\rm dec} \gg \Omega_\Lambda/\Omega_m$. Retaining only the leading term, the approximated optical depth from the residual ionization fraction is estimated to be

$$\tau^{\rm res} \approx 1.24 \times 10^{-6} (1 + z_{\rm dec})^{3/2} \approx 0.045, \quad (2)$$

independent of the cosmological parameters and of the helium fraction. Therefore after last scattering we do not expect any significant effect on CMB anisotropies coming from the primordial helium fraction, until the reionization epoch.

Fairly little is known about the exact reionization mechanism and its redshift dependence (for a review see e.g. [38]). Observation of Gunn-Peterson troughs indicate that the universe was completely ionized after redshift $z \approx 6$, when the universe seemingly completed the reionization [39], possibly for the second time [40]. If temperature information only is available, CMB anisotropies are sensitive only to the integrated reionized fraction, represented by the optical depth, independent of the specific reionization history. However, specific signatures are imprinted on the E-polarization and ET-cross correlation power spectra by the detailed shape of the reionization history (for a detailed discussion, see [41–44]). There are several physically motivated reionization scenarios, which however cannot be clearly distinguished at present [45,46]. In this work we use the most simple model, the sudden reionization scenario: we assume that at the reionization redshift z_r all the hydrogen was quickly reionized, thus producing a sharp rise of n_e from its residual value to n_H. More precisely, z_r is the redshift at which $x_e(z_r) = 0.5$. In our treatment we neglect He II reionization, for which there is evidence at a redshift $z \approx 3$ (see [47] and references therein). This effect is small, since the extra electron released at $z \approx 3$ would change the reionization optical depth by about only 1%. We also neglect the increase of the helium fraction due to nonprimordial helium production, which has

a negligible effect on CMB anisotropies. Those approximations do not affect the results at today's level of sensitivity of CMB data: for WMAP noise levels, even inclusion of the polarization spectra is not enough to distinguish between a sudden reionization scenario and a more complex reionization history. At the level of Planck a more refined modeling of the reionization mechanism will be necessary [44,48].

In the sudden reionization scenario adopted here, the relation between reionization redshift and reionization optical depth, $\tau_{\rm r}$, is given by

$$\tau_{\rm r} = \int_{t_0}^{t_{\rm reion}} n_e c \sigma_T dt \approx 11.3 c \sigma_T \omega_b (1 - Y_p) \int_0^{z_r} \frac{d\eta}{da} dz, \quad (3)$$

where t is physical time, η is conformal time and a the scale factor. Here again, since the number density of reionized electrons scales as $\omega_b(1-Y_p)$, the redshift of reionization is positively correlated with Y_p (for fixed optical depth and baryon density).

As a result of the physical mechanism described above, a 10% change in Y_p has a net impact on the CMB power spectrum at the percent level. The impact on the CMB temperature and polarization power spectra is highlighted in Fig. 3. In the temperature panel, we notice that a larger helium fraction slightly suppresses the peaks because of diffusion damping, while it has no impact on large scales. Polarization is induced by the temperature quadrupole component. When reionization occurs, there is a generation of polarized power on the scale corresponding to the acoustic horizon size at the reionization redshift. This particular signature is called the ''reionization bump,'' and is clearly visible in the bottom panel of Fig. 3 in the $\ell \approx 10$ region. The position of the bump in multipole space scales as $\ell_{\rm bump} \propto \sqrt{z_r}$ [49]. As discussed above, a change in the helium fraction implies a shift of the redshift of reionization for a given (fixed) optical depth, therefore the value of Y_p has an effect on the position of the reionization bump in the polarization power spectrum, but not on its height, which is controlled by the optical depth and is proportional to τ^2. This effect is highlighted in the bottom panel: a 10% change in Y_p induces roughly a 10% change in the position of the bump. The subsequent two oscillatory features for $\ell \lesssim 50$ reflect the displacement of further secondary, reionization induced polarization oscillations. However, since the value of polarized power is very low in that region, such secondary oscillations are very hard to detect precisely. In principle, given an accurate knowledge of the reionization history, the effect of Y_p on the polarization bump would assist into determining the helium abundance. However, our ignorance of the reionization history prevents us from recovering useful information out of the measured reionization bump. The displacement induced by Y_p is in fact degenerate with a partial reionization, or with a more complex reionization history (see [44]). Hence constraints on Y_p come effectively from the damping tail in the $\ell \gtrsim 400$ region of the temperature spectrum, which needs to be measured with very high accuracy.

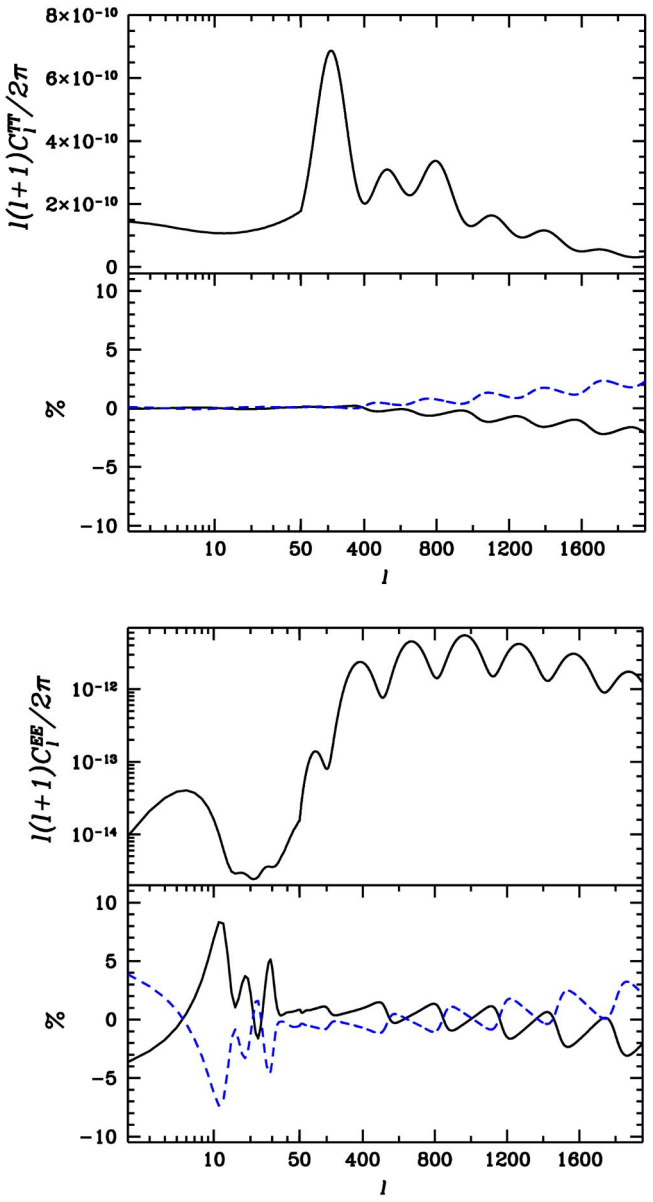

FIG. 3. CMB temperature (top panel) and polarization (bottom panel) power spectra and percentage difference with two different values of the helium fraction for a standard ΛCDM model. The solid-black (dashed-blue) line corresponds to a 10% larger (smaller) value of Y_p with respect to the standard value, $Y_p = 0.24$. All other parameters are fixed to the value of our fiducial model (Table I); in particular, we have $\tau_{\rm r} = 0.166$.

Other light elements like deuterium and helium-3 are much less abundant, and will therefore have even smaller effect on the CMB power spectrum, at the order of 10^{-5}.

B. Monte Carlo analysis

We use a modified version of the publicly available Markov Chain Monte Carlo package COSMOMC [50] as described in [51] in order to construct Markov Chains in our 7 dimensional parameter space. We sample over the following set of cosmological parameters: the physical baryon and CDM den-

sities, $\omega_b \equiv \Omega_b h^2$ and $\omega_c \equiv \Omega_c h^2$, the cosmological constant in units of the critical density, Ω_Λ, the scalar spectral index and the overall normalization of the power spectrum, n_s and A_s (see Sec. III D below for a more precise definition), the redshift at which the reionization fraction is a half, z_r, and the primordial helium mass fraction, Y_p. We restrict our analysis to flat models, therefore the Hubble parameter, $h = H_0/100$ km s^{-1}Mpc^{-1}, is a derived parameter, $h = [(\omega_c + \omega_b)/(1-\Omega_\Lambda)]^{1/2}$. We consider purely adiabatic initial conditions, and we do not include gravitational waves. In the CMB analysis, we assume 3 massless neutrino families and no massive neutrinos. We include the WMAP data [52,53] (temperature and polarization) with the routine for computing the likelihood supplied by the WMAP team [54]. We make use of the CBI [55] and of the decorrelated ACBAR [56,57] band powers above $\ell = 800$ to cover the small angular scale region of the power spectrum.

Since Y_p is a rather flat direction in parameter space with present-day data, we find that a large number of samples is needed in order to achieve good mixing and convergence of the chains in the full 7D space. We use $M = 4$ chains, each containing approximately $N = 3 \times 10^5$ samples. The mixing diagnostic is done on the same lines as in [54], by means of the Gelman and Rubin criterion [58]. The burn-in of the chains also takes longer than in the case where Y_p is held fixed, and we discard 6000 samples per chain.

C. CMB analysis results

Marginalizing over all other parameters, we find that the helium mass fraction from CMB alone is constrained to be $Y_p < 0.647$ at 99% C.L. (1 tail limit), and

$$0.160 < Y_p < 0.501 \tag{4}$$

at 68% C.L. (2 tails). Thus, for the first time the primordial helium mass fraction has been observed using the cosmic microwave background. However, present-day CMB data do not have sufficient resolution to discriminate between the astrophysical helium measurements, $Y_p \sim 0.244$, and the deuterium guided BBN predictions, $Y_p \sim 0.248$, which would require percent precision.

In Fig. 4 we plot the marginalized and the mean likelihood of the Monte Carlo samples as a function of Y_p. If the likelihood distribution is Gaussian, then the 2 curves should be indistinguishable. The difference between marginalized and mean likelihood for Y_p indicates that the marginalized parameters are skewing the distribution, and therefore that correlations play an important role. Although the mean of the 1D marginalized likelihood is rather high, $\langle \mathcal{L}(Y_p) \rangle = 0.33$, the mean likelihood peaks in the region indicated by astrophysical measurements, $Y_p \sim 0.25$. In view of this difference, it is important to understand the role of correlations with other parameters, and we will turn to this issue now.

In Fig. 5 we plot joint 68% and 99% confidence contours in the (ω_b, Y_p) space. From the Monte Carlo samples we obtain a small and negative correlation coefficient between the two parameters $\mathrm{corr}(Y_p, \omega_b) = -0.14$. Baryons and helium appear to be anticorrelated simply because present-day WMAP data do not map the peaks structure to sufficiently

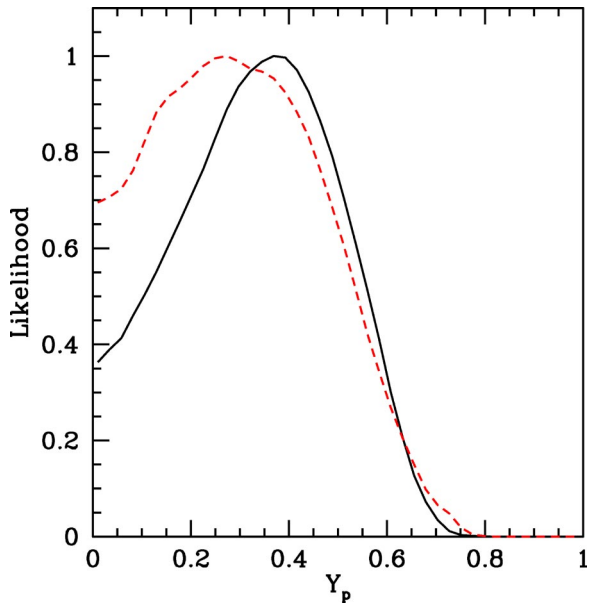

FIG. 4. One-dimensional posterior likelihood distribution for the helium mass fraction, Y_p, using CMB data only. The solid-black line is for all other parameters marginalized; the dashed-red line gives the mean likelihood.

high ℓ. Precise measurements in the small angular scale region should reveal the expected positive correlation between the baryon and helium abundances, which is potentially important in order to correctly combine BBN predictions and CMB measurements of the baryon abundance. We turn to this question in more detail in the next section. In SBBN the baryon fraction and helium fraction are correlated along a

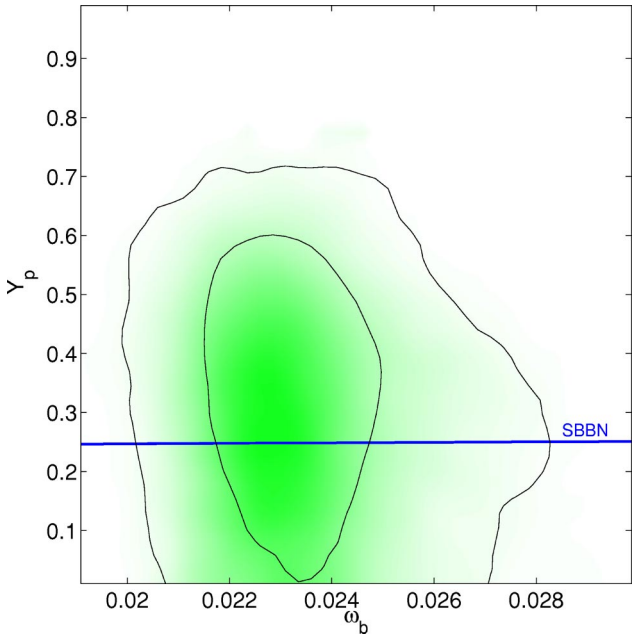

FIG. 5. Joint 68% and 99% confidence contours in the (ω_b, Y_p) plane from CMB data alone. The solid-blue line gives the SBBN prediction [14], which on this figure almost looks like a straight line.

different direction (cf. Fig. 5). However, this correlation is very weak, and the SBBN relation gives practically a flat line. Since the two parameters are not independent from the CMB point of view, it is in fact not completely accurate to do the CMB analysis with fixed helium mass fraction of $Y_p = 0.24$ to get the error bars on the baryon fraction, and then reinput this baryon fraction (and error bars) to predict the helium mass fraction from BBN. The most accurate procedure is to analyze the CMB data leaving Y_p as a free parameter, thereby obtaining the correct (potentially larger) error bars on ω_b upon marginalization over Y_p.

In view of the emerging baryon tension between CMB and BBN, it is important to check whether allowing helium as a free parameter can significantly change the CMB determination of the baryon density or its error. In order to evaluate in detail the impact of Y_p on the error bars for ω_b, we consider the following 3 cases.

(a) The usual case, when the helium fraction for the CMB analysis is assumed to be known *a priori* and is fixed to the canonical value $Y_p = 0.24$.

(b) A case with a weak astrophysical Gaussian prior on the helium fraction, which we take to be $Y_p = 0.24 \pm 0.01$. As discussed above, the error bars of the astrophysical measurements are typically a factor 5 tighter than this, but our prior is chosen to encompass the systematic spread between the different observations.

(c) The case in which we assume a uniform prior for Y_p in the range $0 \leqslant Y_p \leqslant 1$, i.e. Y_p is considered as a totally free parameter.

We do not find any significant change in the error bars for ω_b in the 3 different cases. The confidence intervals on ω_b alone are determined to be [case (c)] $0.0221 < \omega_b < 0.0245$ at 68% C.L. ($0.0204 < \omega_b < 0.0276$ at 99% C.L.). The standard deviation of ω_b as estimated from the Monte Carlo samples is found to be $\hat{\sigma}_b = 1.3 \times 10^{-3}$. This is in complete agreement with the error bars on ω_b obtained by the WMAP team for the standard ΛCDM case [33]. We conclude that at the level of precision of present-day CMB data, it is still safe to treat the baryon abundance and the helium mass fraction as independent parameters. This result is nontrivial, since the fact that the damping tail is not yet precisely measured above the second peak would *a priori* suggest that degeneracies between Y_p, ω_b, and n_s could potentially play a role once the assumption of zero uncertainty on Y_p is relaxed. The impact of Y_p is small enough, and the error bars on ω_b large enough that a uniform prior on Y_p can still be accommodated within the uncertainty in the baryon abundance obtained for case (a). However, the $Y_p - \omega_b$ correlation will have to be taken into account to correctly analyze future CMB data, with a quality such as Planck. We discuss this potential in the next section.

We observe the expected correlation between the redshift of reionization and the helium fraction (Fig. 6), which is discussed above. The correlation coefficient between the two parameters is found to be rather large and positive, $\mathrm{corr}(Y_p, z_r) = 0.40$. This correlation produces a noticeable change in the marginalized 1D-likelihood distribution for z_r as we go from case (a) to case (c). Marginalization over the additional degree of freedom given by Y_p broadens considerably the error bars on z_r. In fact, the 68% confidence interval for z_r increases by roughly 20% (and shifts to somewhat higher values), from 10.2–20.9 [case (a)] to 10.6–23.3 [case (c)]. Case (b) exhibits similar error-bars as case (a). On the other hand, the determination of the reionization optical depth is not affected by the inclusion of helium as a free parameter, giving in all cases $0.08 < \tau_r < 0.23$. Correspondingly, the correlation is less significant, $\mathrm{corr}(Y_p, \tau_r) = -0.11$. We therefore conclude that the differences in the determination of z_r are due only to the variation of the amount of electrons available for reionization as Y_p is changed.

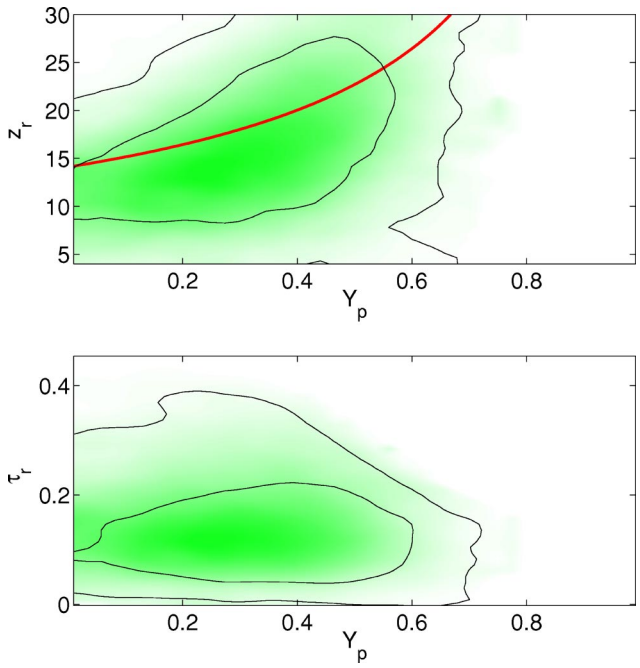

FIG. 6. Joint 68% and 99% confidence contours in the (Y_p, z_r) plane (upper panel) and in the corresponding (Y_p, τ_r) plane (bottom panel) from CMB data alone. In the upper panel, the solid-red line is the relation $z_r(Y_p)$ from Eq. (3), obtained by fixing the reionization optical depth to the value $\tau_r = 0.166$, while the other parameters are the ones of our fiducial ΛCDM model of Table I. Although clearly the exact shape of $z_r(Y_p)$ depends on the particular choice of cosmology, it is apparent that the $Y_p - z_r$ degeneracy is along this direction. The correlation between $Y_p - \tau_r$ is almost negligible with present-day data (bottom panel).

Leaving Y_p as a free parameter also has an impact on the relation between ω_b and the scalar spectral index, n_s. The extra power suppression on small scales which is produced by a larger Y_p can be compensated by a blue spectral index (see Fig. 7).

D. Potential of future CMB observations

In order to estimate the precision with which future satellite CMB measurements will be able to constrain the helium mass fraction we perform a Fisher matrix analysis (FMA). This technique approximates the likelihood function with a Gaussian distribution around a fiducial model, which is as-

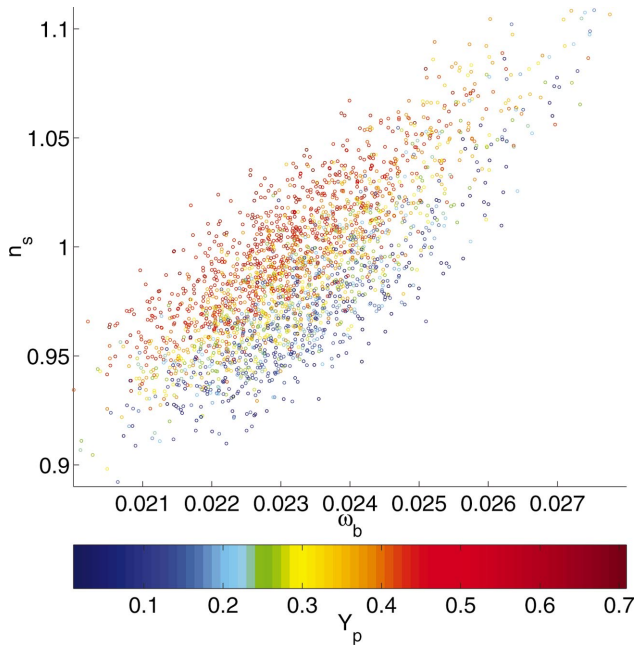

FIG. 7. (Color) Scatter plot in the $\omega_b - n_s$ plane, with the value of Y_p rendered following the color scale. Green corresponds roughly to the SBBN preferred value.

sumed to be the best fit model. The Fisher information matrix F gives the second order expansion of the likelihood around its peak, and it is computed from the derivatives of the power spectrum with respect to the cosmological parameters. The expected performance of the experiment can be modelled with a noise contribution to the likelihood function, which is described in terms of a few experimental parameters. The covariance matrix C is then given by the inverse of the Fisher matrix, $C=F^{-1}$. It is then straightforward to evaluate the expected 1σ error on parameter i, which is given by $\sqrt{c_{ii}}$ (all other marginalized). The main advantage of the FMA is that it gives reliable and accurate predictions (including information on the expected degeneracies) with minimal computational effort. For further details on the Fisher matrix formalism, see e.g. [59–66].

1. Parameters set

In order to obtain a reliable prediction, it is extremely important to choose a parameter set wrt which the dependence of the CMB power spectrum is as linear and uncorrelated as possible. This issue has been discussed exhaustively in Ref. [67], where the authors introduce a set of ''physical parameters'' which satisfies the above requirements. In the present work we retain most of the physical parameters defined in Ref. [67]: the ratio between the sound horizon at decoupling and the angular diameter distance $\mathcal{A}$, the baryon density $\mathcal{B}=\Omega_b h^2$, the energy density in the cosmological constant $\mathcal{V}=\Omega_\Lambda h^2$, the matter-radiation density ratio at decoupling $\mathcal{R}$ and $\mathcal{M}$, which is mainly a function of the matter and radiation content. We adopt a slightly different choice for the physical parameter describing reionization. For adiabatic perturbations, the initial power spectrum of the gauge invariant curvature perturbation ζ is written as

$$P_\zeta(k)=A_s\left(\frac{k}{k_0}\right)^{n_s-1}$$

(and we do not take running into account). The quantity ζ corresponds to the intrinsic curvature perturbation on comoving hypersurfaces, and at the end of inflation is related to the gravitational potential perturbation, Ψ, by $\zeta=\frac{3}{2}\Psi$ (see e.g. [68] for more details). We take the pivot-scale k_0 to be $k_0=0.05\ \mathrm{Mpc}^{-1}$. If τ_r denotes the optical depth to reionization, then defining $\mathcal{T}=A_s\exp(-2\tau)$ is a good way to take into account the degeneracy between the optical depth and normalization. Our parameter set contains then the six above physical parameters $(\mathcal{A},\mathcal{B},\mathcal{V},\mathcal{R},\mathcal{M},\mathcal{T})$, the power spectrum normalization A_s, the scalar spectral index n_s and the helium fraction Y_p.

The choice of the physical parameter set makes it easy to implement in the FMA interesting theoretical priors. For instance, we are interested in imposing flatness in our forecast, in order to be able to directly compare present-day accuracy on Y_p with the potential of Planck and CVL. The prior on the curvature of the universe is imposed in the FMA by fixing the value of the parameter $\mathcal{A}$ to the one of the fiducial model. In fact, the parameter $\mathcal{A}$ is a generalization of the shift parameter, which describes the sideway shift of the acoustic peak structure of the CMB power spectrum as a function of the geometry of the universe and its content in matter, radiation and cosmological constant. Although imposing $\mathcal{A}=\text{const}$ is not the same as having curvature=constant over the full range of cosmological parameters, for the purpose of evaluating derivatives the two conditions reduce to the same. The fact that our fiducial model is actually slightly open (see below), does not make any substantial difference in the results, apart from reducing the numerical inaccuracies which would arise had we computed the derivatives around an exactly flat model. We can also easily impose a prior knowledge of the helium fraction, by fixing the value of Y_p, as it is usually done in present CMB analysis, and investigate how this modifies the expected error on the baryon density.

2. Accuracy issues

We numerically compute double sided derivative of the power spectrum around the fiducial model with cosmological parameters given in Table I. We find it necessary to increase the accuracy of CAMB by a factor of 3 in each of the ''accuracy boost'' values. As a fiducial model, we use the best fit model to the WMAP data for the standard ΛCDM scenario, as given in Table 1 of Ref. [33]. However, in order to avoid numerical inaccuracies which arise when differentiating around a flat model, we reduce slightly the value of Ω_Λ by imposing an open universe, $\Omega_{\mathrm{tot}}=0.99$. We perform the FMA for the expected capabilities of Planck's High Frequency Instrument (HFI) and for an ideal CMB measurement which would be cosmic variance limited (CVL) both in temperature and in E-polarization (and we do not consider the B-polarization spectrum), and therefore represents the best possible parameter measurement from CMB anisotropies alone. The complicated issues coming from foreground removals, point source subtractions, etc. are assumed to be

TABLE I. Cosmological parameters for the fiducial ΛCDM model around which the FMA is performed. We choose a slightly open model to avoid numerical inaccuracies in the derivatives.

Baryons	Ω_b	0.046
Matter	Ω_m	0.270
Dark energy	Ω_Λ	0.720
Radiation	$\Omega_{\rm rad}$	7.95×10^{-3}
Massless ν families	N_ν	3.04
Total density	$\Omega_{\rm tot}$	0.990
Hubble constant	h	0.72
Optical depth	$\tau_{\rm r}$	0.166
Spectral index	n_s	0.99
Normalization	A_s	2×10^{-9}

already (roughly) taken into account in the experimental parameters for the experiment. Those are the effective percentual sky coverage $f_{\rm sky}$, the number of channels, the sensitivity of each channel $\sigma_c^{T,E}$ for temperature (T) and E-polarization (E) in μK and the angular resolution $\theta_c^{T,E}$ (in arcmin). For Planck HFI, we take the 3 channels with frequencies 100, 143 and 217 GHz, with respectively $\sigma^T_{c=1,2,3}=5.4,6.0,13.1$ and $\sigma^E_{c=2,3}=11.4,26.7$ and we have $f_{\rm sky}=0.85$ [69]. Since the CVL is an ideal experiment, we put its noise to zero and assume perfect foregrounds removal, so that $f_{\rm sky}=1$. In order to test the accuracy of our predictions and compare present-day results with the forecasts, we also perform an FMA with WMAP first year parameters, obtaining excellent agreement between the FMA results and the error bars from actual data. For the purpose of comparison, we include forecasts for the full WMAP 4 years mission, which will also measure E-polarization and reduce present-day errors on the temperature spectrum by a factor of 2. We limit the range of multipoles to $\ell<2000$, because at smaller angular scales nonprimary anisotropies begin to dominate (Sunyaev-Zeldovich effect). The authors of Ref. [70] discuss the issue of numerical precision of 3 different CMB codes and conclude that they are accurate to within 0.1%. While this is encouraging, it is not of direct relevance to this work, since what matters in the computation of derivatives is not much the absolute precision of the spectra, but rather their relative accuracy.

3. Forecasts and discussion

Table II summarizes our forecasts for the future measurements and compares them with the results obtained from WMAP actual data.

We notice that when the WMAP full 4 years data will be available (including E-polarization), the error on the baryon density is expected to decrease by a factor of 2 to 2.86%, compared to today's 5.04% (assuming flatness). Nevertheless, inclusion of Y_p as a free parameter will still have no effect on the determination of ω_b for WMAP, i.e. Y_p will remain an essentially flat direction when marginalized over. While the determination of the helium fraction will improve, the FMA cannot reliably assess quantitatively how much, since for such large errors the likelihood distribution is not Gaussian and the quadratic approximation breaks down. In the table we therefore give the FMA estimation as an indication, with the caveat that the Fisher approximation is likely to be inaccurate for the real errors on Y_p from WMAP's 4 years data.

It is interesting that for Planck the effect of the helium fraction can no longer be neglected. Inclusion of the helium fraction increases the error on ω_b by roughly 80%, from 0.70% to 1.26%. The correlation between the two parameters will have to be taken into account, as is evident from Fig. 8. The expected correlation coefficient is $\mathrm{corr}(Y_p,\omega_b)=0.84\ (0.91)$ for Planck (for CVL). The expected $1-\sigma$ er-

TABLE II. Fisher matrix forecasts and comparison with present-day results, for different priors and using different combinations of temperature and polarization CMB spectra. Errors are in percent with respect to the values of the fiducial model, $Y_p=0.24$ and $\omega_b=0.0238$ (1-σ C.L. all others marginalized).

	Temperature, TE-cross, E-polarization				
	No priors		Flatness		Flatness and $Y_p=0.24$
	$\frac{\Delta Y_p}{Y_p}$	$\frac{\Delta\omega_b}{\omega_b}$	$\frac{\Delta Y_p}{Y_p}$	$\frac{\Delta\omega_b}{\omega_b}$	$\frac{\Delta\omega_b}{\omega_b}$
WMAP 4 yrs [a]	~50	2.92	~40	2.86	2.86
Planck	7.60	1.31	4.96	1.26	0.70
CVL	2.59	0.34	1.52	0.32	0.13
	Temperature+TE-cross				
WMAP 1st yr [b]	N/A	N/A	71.25	5.04	5.04
WMAP 4 yrs [a]	~75	4.10	~60	3.94	3.94
Planck	8.91	1.74	6.60	1.63	0.74
CVL	5.18	0.55	2.84	0.55	0.19

[a]FMA forecast, 4 years mission including E-polarization.

[b]Actual WMAP data and other CMB experiments, this work.

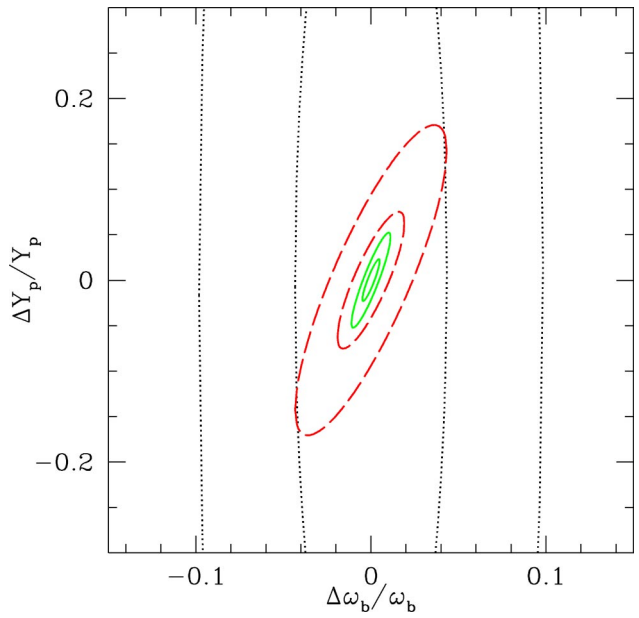

FIG. 8. FMA forecast for the expected errors from WMAP 4 years mission (dotted-black), Planck (dashed-red) and a CVL experiment (solid-green). The ellipses encompass 1-σ and 3-σ joint confidence regions for $\omega_b - Y_p$ (all other parameters marginalized). The axis values give the error with respect to the fiducial model values. This forecast is for the full CMB information (temperature, TE-cross, E-polarization) and assumes flatness.

ror on Y_p is about 5% for Planck, or $\Delta Y_p \sim 0.01$. This is of the same order as the spread in current astrophysical measurements. We conclude that in Planck-accuracy data analysis it will be necessary to include the uncertainty in the determination of the helium mass fraction, at least in the form of a Gaussian prior over Y_p of the type we used in the CMB data analysis presented above.

Finally, measuring CMB temperature and polarization with cosmic variance accuracy would allow to constrain Y_p to within 1.5%, or $\Delta Y_p \sim 0.0036$ (assuming flatness). Such an ideal measurement would be able to discriminate between the BBN-guided, deuterium based helium value and the current lowest direct helium observations (cf. Fig. 1).

Our forecasts for the uncertainty in the helium mass fraction from future observations are in excellent agreement with the findings of Ref. [71]. There, the standard deviation on Y_p for Planck is estimated to be $\Delta Y_p = 0.012$. The authors of Ref. [71] also consider an experiment (CMBPol) with characteristics similar to our CVL, for which they forecast $\Delta Y_p = 0.0039$, again in close agreement with our result. An earlier work [72] found for Planck (temperature and polarization) $\Delta Y_p = 0.013$, in satisfactory concordance with our result. It should be noticed that the forecast reported for MAP in Table 2 of Ref. [72], namely $\Delta Y_p = 0.02$, is nothing but the Gaussian prior $Y_p = 0.24 \pm 0.02$ which was assumed in their analysis.

The main source of improvement for the determination of Y_p will be the better sampling of the temperature damping tail provided by Planck and the CVL. Polarization measurements have mainly the effect of reducing the errors on other parameters. In fact, we have checked that excluding from our FMA the $2 \leqslant \ell \leqslant 50$ region of the E-polarization and ET-correlation spectra changes the forecast precision on Y_p less than about 10–15 % for Planck and less than a few percent for CVL. This supports the conclusion that the low-ℓ reionization bump is not very useful in measuring the helium abundance, because of the degeneracy with z_r.

IV. CONCLUSIONS

We have analyzed the ability of CMB observations to determine the helium mass fraction, Y_p. We find that present data only allow a marginal detection, $0.160 < Y_p < 0.501$ at 68% C.L. This determination is completely independent from the usual astrophysical observations and uses CMB data only. We discuss degeneracies between Y_p and other cosmological parameters, most notably the baryon abundance, the redshift and optical depth of reionization and the spectral index. We conclude that present-day CMB data accuracy does not require the inclusion of Y_p as a free parameter. We find that Planck will determine the helium mass fraction within 5% (or $\Delta Y_p \sim 0.01$), which however will only allow a marginal discrimination between different astrophysical measurements. Nevertheless, we point out that the uncertainty of the helium fraction will have to be taken into account in order to correctly estimate the errors on the baryon density from Planck. To determine if the emerging baryon tension (from BBN) is related to underestimated systematic error-bars or whether it is an indication of new physics, CMB observation will have to be pushed very close to the cosmic variance limit in both temperature and polarization.

ACKNOWLEDGMENTS

It is a pleasure to thank Ruth Durrer, Lloyd Knox, Samuel Leach, Anthony Lewis, Christophe Ringeval, Dominik Schwarz and Gary Steigman for useful comments and discussions. This work was performed on the SUN Enterprise 10000 Supercomputer owned and operated by the University of Geneva. R.T. is partially supported by the Swiss National Science Foundation, the Schmidheiny Foundation and the European Network CMBNET. S.H. thanks the Tomalla foundation for support.

[1] R.H. Cyburt, B.D. Fields, and K.A. Olive, Phys. Lett. B **567**, 227 (2003).
[2] E.W. Kolb and M.S. Turner, *The Early Universe*, Frontiers in Physics Vol. 69 (Addison-Wesley, Redwood City, CA, 1990), p. 547.
[3] D. Kirkman, D. Tytler, N. Suzuki, J.M. O'Meara, and D. Lubin, astro-ph/0302006.
[4] M. Pettini and D.V. Bowen, Astrophys. J. **560**, 41 (2001).
[5] Y.I. Izotov and T.X. Thuan, Astrophys. J. **500**, 188 1998).
[6] K.A. Olive, G. Steigman, and E.D. Skillman, Astrophys. J.

483, 788 (1997).
[7] A. Peimbert, M. Peimbert, and V. Luridiana, Astrophys. J. **565**, 668 (2002).
[8] V. Luridiana, A. Peimbert, M. Peimbert, and M. Cervino, Astrophys. J. **592**, 846 (2003).
[9] Y.I. Izotov, F.H. Chaffee, C.B. Foltz, R.F. Green, N.G. Guseva, and T.X. Thuan, Astrophys. J. **527**, 757 (1999).
[10] V. Barger, J.P. Kneller, H.S. Lee, D. Marfatia, and G. Steigman, Phys. Lett. B **566**, 8 (2003).
[11] S.G. Ryan, T.C. Beers, K.A. Olive, B.D. Fields, and J.E. Norris, Astrophys. J. Lett. **530**, L57 (2000).
[12] M. Salaris and A. Weiss, astro-ph/0104406.
[13] N. Hata *et al.*, Phys. Rev. Lett. **75**, 3977 (1995).
[14] S. Burles, K.M. Nollett, and M.S. Turner, Astrophys. J. Lett. **552**, L1 (2001).
[15] S.H. Hansen, G. Mangano, A. Melchiorri, G. Miele, and O. Pisanti, Phys. Rev. D **65**, 023511 (2002).
[16] M.H. Pinsonneault, T.P. Walker, G. Steigman, and V.K. Narayanan, Astrophys. J. **527**, 180 (1999).
[17] M.H. Pinsonneault, G. Steigman, T.P. Walker, and V.K. Narayanan, Astrophys. J. **574**, 398 (2002).
[18] R.E. Lopez and M.S. Turner, Phys. Rev. D **59**, 103502 (1999).
[19] S. Esposito, G. Mangano, G. Miele, and O. Pisanti, Nucl. Phys. **B568**, 421 (2000).
[20] S. Esposito, G. Mangano, G. Miele, and O. Pisanti, J. High Energy Phys. **09**, 038 (2000).
[21] A. Cuoco, F. Iocco, G. Mangano, G. Miele, O. Pisanti, and P.D. Serpico, astro-ph/0307213.
[22] A.D. Dolgov, S.H. Hansen, S. Pastor, and D.V. Semikoz, Nucl. Phys. **B548**, 385 (1999).
[23] A.D. Dolgov, S.H. Hansen, G. Raffelt, and D.V. Semikoz, Nucl. Phys. **B590**, 562 (2000).
[24] P. Di Bari and R. Foot, Phys. Rev. D **63**, 043008 (2001).
[25] D.P. Kirilova, Astropart. Phys. **19**, 409 (2003).
[26] X.D. Shi, G.M. Fuller, and K. Abazajian, Phys. Rev. D **60**, 063002 (1999).
[27] A.D. Dolgov and F.L. Villante, hep-ph/0308083.
[28] P. Crotty, J. Lesgourgues, and S. Pastor, Phys. Rev. D **67**, 123005 (2003); E. Pierpaoli, Mon. Not. R. Astron. Soc. **342**, L63 (2003); S. Hannestad, J. Cosmol. Astropart. Phys. **05**, 004 (2003); P. Di Bari, Phys. Rev. D **67**, 127301 (2003); S. Pastor, hep-ph/0306233.
[29] R.E. Lopez, S. Dodelson, A. Heckler, and M.S. Turner, Phys. Rev. Lett. **82**, 3952 (1999); S. Hannestad and J. Madsen, Phys. Rev. D **52**, 1764 (1995); A.D. Dolgov, S.H. Hansen, and D.V. Semikoz, Nucl. Phys. **B503**, 426 (1997); A.D. Dolgov, S.H. Hansen, and D.V. Semikoz, Surv. High Energy Phys. **13**, 203 (1998); G. Mangano, G. Miele, S. Pastor, and M. Peloso, Phys. Lett. B **534**, 8 (2002).
[30] H.S. Kang and G. Steigman, Nucl. Phys. **B372**, 494 (1992); J. Lesgourgues and S. Pastor, Phys. Rev. D **60**, 103521 (1999).
[31] A.D. Dolgov *et al.*, Nucl. Phys. **B632**, 363 (2002); Y.Y. Wong, Phys. Rev. D **66**, 025015 (2002); K.N. Abazajian, J.F. Beacom, and N.F. Bell, *ibid.* **66**, 013008 (2002).
[32] V. Barger, J.P. Kneller, P. Langacker, D. Marfatia, and G. Steigman, Nucl. Phys. **B569**, 123 (2003).
[33] D.N. Spergel *et al.*, Astrophys. J., Suppl. Ser. **178**, 175 (2003).
[34] Iu.E. Liubarskii and R.A. Sunyaev, Astron. Astrophys. **123**, 171 (1983).
[35] W. Hu, D. Scott, N. Sugiyama, and M.J. White, Phys. Rev. D **52**, 5498 (1995).
[36] S. Seager, D.D. Sasselov, and D. Scott, Astrophys. J., Suppl. Ser. **128**, 407 (2000).
[37] S. Seager, D.D. Sasselov, and D. Scott, Astrophys. J. Lett. **523**, L1 (1999).
[38] Z. Haiman, in *Carnegie Observatories Astrophysics Series, Vol. 1*, edited by L. C. Ho (Cambridge University Press, Cambridge, England, in press), astro-ph/0304131.
[39] R.H. Becker *et al.*, Astron. J. **122**, 2850 (2001); X. Fan *et al.*, *ibid.* **123**, 1247 (2002).
[40] R. Cen, Astrophys. J. **591**, 12 (2003); L. Hui and Z. Haiman, astro-ph/0302439.
[41] M. Bruscoli, A. Ferrara, and E. Scannapieco, Mon. Not. R. Astron. Soc. **330**, 43 (2002).
[42] W. Hu and G.P. Holder, Phys. Rev. D **68**, 023001 (2003).
[43] M. Kaplinghat *et al.*, Astrophys. J. **583**, 24 (2003).
[44] G.P. Holder *et al.*, Astrophys. J. **595**, 13 (2003).
[45] Z. Haiman and G.P. Holder, Astrophys. J. **595**, 1 (2003).
[46] S.H. Hansen and Z. Haiman, astro-ph/0305126.
[47] T. Theuns *et al.*, Astrophys. J. Lett. **574**, L111 (2002).
[48] A.G. Doroshkevich, I.P. Naselsky, P.D. Naselsky, and I.D. Novikov, Astrophys. J. **586**, 709 (2003).
[49] M. Zaldarriaga, Phys. Rev. D **55**, 1822 (1997).
[50] http://cosmologist.info/cosmomc/
[51] A. Lewis and S. Bridle, Phys. Rev. D **66**, 103511 (2002).
[52] A. Kogut *et al.*, Astrophys. J., Suppl. Ser. **148**, 161 (2003).
[53] G. Hinshaw *et al.*, astro-ph/0302222.
[54] L. Verde *et al.*, astro-ph/0302218.
[55] T. Pearson *et al.*, Astrophys. J., Suppl. Ser. **148**, 195 (2003).
[56] http://cosmologist.info/ACBAR.
[57] C.L. Kuo *et al.*, astro-ph/0212289.
[58] A. Gelman and D. Rubin, Stat. Sci. **7**, 457 (1992).
[59] L. Knox, Phys. Rev. D **52**, 4307 (1995).
[60] G. Efstathiou and J.R. Bond, Mon. Not. R. Astron. Soc. **304**, 75 (1999).
[61] R.J. Bond, G. Efstathiou, and M. Tegmark, Mon. Not. R. Astron. Soc. **291**, L33 (1997).
[62] R. Bowen, S.H. Hansen, A. Melchiorri, J. Silk, and R. Trotta, Mon. Not. R. Astron. Soc. **334**, 760 (2002).
[63] C.J. Martins, A. Melchiorri, R. Trotta, R. Bean, G. Rocha, P.P. Avelino, and P.T. Viana, Phys. Rev. D **66**, 023505 (2002).
[64] C.J. Martins, A. Melchiorri, G. Rocha, R. Trotta, P.P. Avelino, and P. Viana, astro-ph/0302295.
[65] M. Zaldarriaga and U. Seljak, Phys. Rev. D **55**, 1830 (1997).
[66] M. Tegmark, A.N. Taylor, and A.F. Heavens, astro-ph/9603021.
[67] A. Kosowsky, M. Milosavljevic, and R. Jimenez, Phys. Rev. D **66**, 063007 (2002).
[68] R. Durrer, J. Phys. Stud. **5**, 177 (2001).
[69] Planck Homepage, http://astro.estec.esa.nl/Planck
[70] U. Seljak, N. Sugiyama, M. White, and M. Zaldarriaga, Phys. Rev. D **68**, 083507 (2003).
[71] M. Kaplinghat, L. Knox, and Y.-S. Song, Phys. Rev. Lett. **91**, 241301 (2003).
[72] D. Eisenstein, W. Hu, and M. Tegmark, Astrophys. J. **518**, 2 (1998).